Full Length Article

Information hidden behind a single peak in the C 1s spectrum of graphene on Ir(111)

Cecilia Botta [a], Federico Loi [a], Dario Alfè [b,c], Alessandro Baraldi [a,d,*]

[a] Department of Physics, University of Trieste, Via Valerio 2, 34127 Trieste, Italy
[b] Department of Earth Sciences and London Centre for Nanotechnology, University College London, Gower Street, London WC1E 6BT, UK
[c] Dipartimento di Fisica Ettore Pancini, Università di Napoli Federico II, Monte S. Angelo, Napoli 80126, Italy
[d] Elettra Sincrotrone Trieste, AREA Science Park, 34149 Trieste, Italy

ARTICLE INFO

ABSTRACT

The energy resolution that can be achieved in x-ray photoelectron spectroscopy experiments allows to disentangle the contribution arising from the presence of a large variety of surface atoms in non-equivalent configurations which manifests itself not only with the appearance of different spectral components, but also as unusual lineshape.

In the present work, we show that the fit of the C 1s core level spectrum of graphene grown on Ir(111) realized using 200 peaks based on *ab initio* calculations, accounting for the non-equivalent C in the (10×10) moiré cell, does not improve the fit quality with respect to the use of a single component. On the contrary, the quantitative fit quality can be drastically increased by introducing a dependency of the Lorentzian width on the distance between C and Ir first-layer atoms. This result is associated to the different electronic properties, and in particular to the different density of states of the σ and π bands, of C atoms sitting on TOP (hills) or FCC (valleys) regions of graphene which affect the lifetimes of the core-holes generated during the photoemission process.

1. Introduction

High-Resolution X-ray Photoelectron Spectroscopy (HR-XPS) has always been, since the pioneering works by Kai Siegbahn [1], one of the most exploited techniques in surface science. With the advent of the massive family of 2D materials [2,3] this experimental approach gained even more attention [4] thanks to its huge surface sensitivity which makes it particularly suitable to investigate the physical and chemical properties of this new fascinating class of materials. Among them, graphene is one of the most studied by using XPS, as testified by the more than 10.000 publications [5] where this technique has been adopted to measure the C 1s core levels in graphene-based systems.

Graphene-metal interfaces, where graphene is grown via chemical vapor deposition, are no exception. They have been widely studied by means of XPS to investigate the nature of the interaction between the carbon layer and the different underlaying metals which greatly affects the electronic properties of the supported graphene itself. Similarly, from the C 1s core level of graphene it is possible to obtain information on a large variety of its chemical properties when it bonds to atoms and molecules which can be used, for instance, to tune its doping [6,7] or to evaluate its adsorption and reaction properties [8,9].

Single-layer graphene epitaxially grown on the Ir(111) surface by the exposure to hydrocarbons such as ethylene at temperatures higher than 1300 K is a model example of quasi-free standing graphene [10]. This interface was used to highlight the dominant role played by van der Waals dispersion forces in the graphene-metal interaction [11,12], to induce a band gap opening by doping graphene with hydrogen atoms [13], and to showcase the energy dispersion effects that can be observed also in deep core levels [14]. The first major work involving HR-XPS measurement on the core-levels of epitaxial graphene by Preobrajenski *et al.* [15] showed that in the case of surfaces with which graphene has the weakest interaction, such as Pt(111) and the aforementioned Ir (111), the C 1s core level spectrum is composed of a single component centered at about 284.1 eV. On the contrary, when the graphene-metal interaction is strong enough to induce a partial rehybridization of the C atoms and in the presence of a large lattice mismatch (as in the case of Ru(0001) [15–18]), the highly corrugated morphology of the single-atom layer results in a C 1s spectrum which is apparently split into two components. The one with the highest binding energy (BE) originates from those atoms which strongly interact with and are closer to the

substrate (down to about 2 Å), while the component at lower BE corresponds to the C atoms sitting further away from the metallic surface. Later studies highlighted that when epitaxial graphene is highly corrugated, as it happens when it is grown on the (0001) surfaces of rhenium [19] and ruthenium [20], the double-peak structure arises from an extremely large distribution of the C 1s core level BEs due to the large number of non-equivalent atoms in the unit cell. For instance, graphene on Re(0001) forms a moiré lattice with a (11x11) periodic carbon unit cell which overlaps with a (10x10) unit cell of the metallic substrate. This structure implies the presence of 242 nonequivalent C atoms which, based on their distance from the Re(0001) surface, build up the double-peak distribution of the BEs [19]. Theoretical calculations on the C 1s core levels based on DFT formalisms, which include final-state effects, allowed to replicate with great accuracy the experimental lineshape when, besides the BEs, also the phonon and experimental broadening (Gaussian contribution) and the intrinsic broadening related to the finite lifetime of the core–hole (Lorentzian contribution) are considered.

In this work, we aim to understand whether also in the limit case where the C 1s spectrum appears as a single component, such as for the graphene/Ir(1 1 1) interface, it is possible to obtain high-quality fit of the experimental spectrum by considering the presence of several non-equivalent C atoms. As a matter of fact, the C 1s core level spectrum of graphene/Ir(1 1 1) has already been qualitatively analyzed by using 200 components due to the presence of the (10 x 10) unit cell that graphene forms on a (9 x 9) Ir(1 1 1) [21].

In our quantitative reduced-χ^2 analysis based on calculated core electron binding energies including final-state effects we show that the fit of the C 1s spectrum of Gr/Ir(1 1 1) performed by using 200 Doniach-Šunjić [22] peaks of equal lineshapes fails to accurately reproduce the experimental spectrum if compared to the fit performed using a single component, which returns a lower reduced-χ^2. It is only the introduction of a functional dependence of the Lorentzian width on the C-Ir distance that allows us to considerably decrease the reduced-χ^2 by a factor of 2. These findings are discussed in terms of different electronic structure of the C atoms sitting close (valleys region) or far (hills region) from the metallic substrate resulting in different relaxation time of the core-holes generated in the photoemission process.

2. Methods

2.1. Experimental details

HR-XPS measurements were performed at the SuperESCA beamline of the Elettra synchrotron facility in Trieste, Italy. The Ir(1 1 1) single crystal used for the graphene growth was first cleaned through several cycles of Ar$^+$ sputtering and annealing up to 1470 K, followed by exposure to oxygen (three ramps up to 1070 K with an O$_2$ pressure of 5 x 10^{-7} mbar) to remove residual C atoms. The residual O was finally removed by making it react with H$_2$ in a temperature range between 370 and 770 K and with a pressure of 1 x 10^{-7} mbar. A final flash up to 570 K was then sufficient to remove the small amount of residual H.

The cleanliness of the Ir surface was checked by measuring the Ir 4f$_{7/2}$ core level, which showed the typical surface core level shift to lower binding energies, equal to −550 meV [23], and by verifying the presence of contaminants such as C, O, S and B. The low electron energy diffraction image of the surface acquired after the cleaning procedure showed the presence of a (1x1) structure with bright and sharp diffraction spots with a low background. Graphene was subsequently grown by following a well-established procedure [24]. In particular, the Ir(1 1 1) surface was exposed to an initial pressure of 5 x 10^{-8} mbar of C$_2$H$_4$ at a temperature of 470 K for 2 min. This first step is followed by five temperature ramps between 200 and 1420 K. Finally, two final temperature ramps were performed with an increased 5 × 10^{-8} mbar background pressure to fill the last holes in the graphene layer, since the growth follows a self-limiting process. The graphene layer obtained by following this procedure showed a low electron energy diffraction

pattern with new diffraction spots arising from a (10x10) unit cells of graphene (which correspond to the dimension of the moiré unit cell) on (9x9) cells of the Ir(1 1 1) substrate, in a ratio of surface unit cell vectors equal to 1.111, in agreement with first reports [10]. The mismatch between the lattice vectors of graphene and Ir results in the formation of a moiré lattice superstructure.

The C 1s spectrum of graphene was fitted by using the most adopted lineshapes in literature: simple Gaussian and Lorentzian functions, their convolution (Voigt function) and a Doniach-Šunjić function convoluted with a Gaussian width which accounts for phonon, instrumental and inhomogeneous broadening (being G the Gaussian width). The DS profile contains a Lorentzian distribution (being L the Lorentzian width) arising from the finite core–hole lifetime and an asymmetry parameter α (for electron-hole pair excitations near the Fermi level and π*—> π* interband transitions which are known to vary with the degree of graphene doping [25]. Lineshape parameters obtained are based on least-squares fit.

2.2. Theoretical calculations

The DFT calculations were performed as implemented in the Vienna Ab-initio Simulation Package (VASP) code [26]. The system was described with a slab composed of 4 layers of Ir in a (9 x 9) hexagonal supercell and a layer of (10 x 10) unit cell of graphene placed on top of them. The bottom two layers of Ir were kept frozen at their bulk geometry, with a lattice parameter of 2.74 Å, and the rest of the system was fully relaxed using the rev-vdwDF2 functional [27] until the largest residual force was less than 0.015 eV/Å. We employed the projector augmented method (PAW) [28,29] using PBE potentials [30]. The plane wave cutoff was set to 400 eV, and the relaxations were performed by sampling the Brillouin zone using the Γ point only. To obtain the partial density of states, we have performed single point DFT calculations in 512 K points of the K-space, using the geometries obtained with the rev-vdw-DF2 functional.

Core level binding energies (CLBE) are obtained as the difference in energy from two calculations. The first is a standard calculation, and the second is a calculation in which a core electron is removed from an atom and placed in valence. This can be achieved by creating a new pseudo potential for the atom with the core hole and adding one electron to the total number of valence electrons. In the PAW formalism employed in VASP this is done during the calculation, without the need to explicitly generate a separate PAW for the atom with the hole in the core. In both calculations the total charge density is driven to self-consistency, thereby taking into account the relaxation of the valence electrons around the hole. The other core electrons are kept frozen, and so their screening is neglected. This is commonly known as the 'final state' approximation. The absolute values of the CLBEs obtained in these calculations cannot be related to measurable quantities, but differences in CLBEs can usually be obtained with accuracies of a few tens of meV. Absolute core level BEs are shifted by using an offset parameter which is included in the fitting procedure and allowed to vary until the best fit with the experiment is found.

3 Results

3.1. 3.1 Experimental results

The C 1s spectrum in Fig. 1 corresponds to the C single-layer grown with the procedure previously described and measured with a photon energy of 400 eV. The overall resolution, which considers both the resolution of the electron energy analyzer and the spectral broadening of the photon beam, is 50 meV. The experimental standard error associated to the electron counts for each data point is given by the square root of the sum of counts. The spectrum was acquired in normal emission, with the photon beam impinging at the grazing incidence of 20° with respect to the sample plane and an overall acceptance angle of 5°. In these
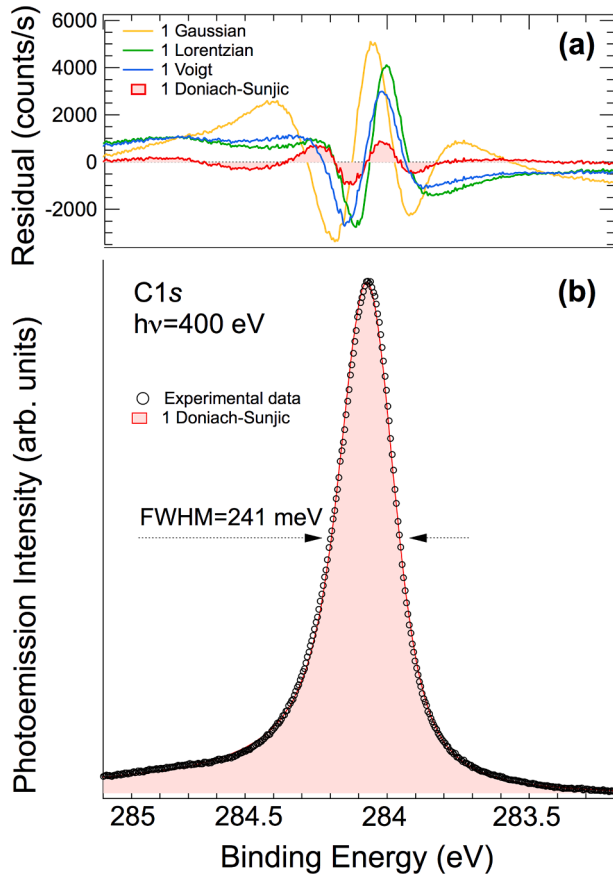
Fig. 1. C 1s spectrum measured at normal emission and at T = 100 K with a photon energy of 400 eV (empty circles) together with the result of the fit performed using a single DS function convoluted with a Gaussian (blue solid line). In the top panel the residual of the fits performed using a single Gaussian (orange curve), a Lorentzian (green curve) and the DSG (blue curve) are reported.

conditions, at the center of the first Brillouin region, it is always possible to measure only the C 1s bonding component, since the anti-bonding state can be observed only at the center of the second Brillouin zone, as it has demonstrated in earlier works [14,31].

The spectrum was measured at T = 100 K to minimize the Gaussian broadening related to phonon excitations. The Full Width al Half Maximum (FWHM) is found to be 241 ± 2 meV, in agreement with previous determination on the same system [21]. To evaluate the quality of a fit, the χ^2 value was used. The χ^2 value is defined as

$$\chi^2 = \sum_{i=1}^{n} \left(\frac{o_i - e_i}{w_i} \right)^2$$

where o_i is the electron counts for each data point, e_i is the electron counts that were expected according to the fitting function, and w_i is the experimental standard error associated with o_i, which corresponds to the square root of the counts [32]. To compare the results also for fitting lineshapes with a different number of parameters, we utilized the reduced-χ^2, which is obtained by dividing the χ^2 value associated to each fit by the number of degrees of freedom:

$$\chi_r^2 = \frac{\chi^2}{n - n_p}$$

where n is the number of data points, n_p is the number of free parameters of the fitting function, and $n - n_p$ is the number of degrees of freedom of the fit.

A preliminary fitting procedure was performed by using a Gaussian

(G) and a Lorenztian (L) lineshape. In both cases, the residual lines (orange for G and green for L) show an evident modulation, which indicates the inadequacy of this analysis. This is also supported by the extremely high reduced-χ^2 values obtained with the two fitting analysis, which are 458.8 and 238.9, respectively. Also the fit done using a Voigt function show a large reduced-χ^2 value (215.39). On the contrary, the fit performed by using the DS function convoluted with a Gaussian, which is the lineshape typically adopted to fit this type of spectra, returns a much better agreement with the experimental line. The best fitting parameters correspond to an L width of 140 meV, a G width of 135 meV and an asymmetry parameters α equal to 0.073. The peak is centered at a binding energy of 284.06 eV. All these values are in excellent agreement with those reported in literature for previous works on the same system [12,14,15,21].

However, it can be appreciated in the top panel of Fig. 1, although the amplitude of the fluctuations of the residual line is lower than in the fit performed with a G or L lineshape, it still shows a modulation, thus suggesting that the reduced-χ^2 value, which now is equal to 10.14, can still be improved.

3.2. Theoretical results

We performed DFT calculations by following a similar procedure than for the analysis of the C 1 s spectrum of Re(0001) [19], Ru(0001) [20], and intercalated systems on Ir(111) and Ru(0001) [12]. As a matter of fact, although graphene grown on Ir(111) is generally considered a weakly corrugated system [33], the atoms in the unit cell are not equivalent with each other and the core level electrons could be affected by the different interaction with the metallic surface in the different regions of the moiré cell.

The graphene layer shows, as expected, a low corrugation. This can be quantified by considering the height h of each C atom with respect to the Ir(111) plane [11]. According to our calculations, this value ranges from 3.30 up to 3.72 Å, with a mean value of 3.47 Å and a standard deviation $\sigma_h = 0.11$ Å, in good agreement with the experimental results by Busse et al. (mean value of 3.38 ± 0.02 Å and $\sigma_h < 0.27 ± 0.04$) Å) [11]. These results show, as it was already discussed by Coraux et al. [34], that the minimum graphene-substrate distance corresponds to the FCC and HCP regions (indicated in Fig. 2a), which are labeled after the position of the center of the graphene hexagons with respect to the Ir (111) surface adsorption sites. On the contrary, the highest distance corresponds to the TOP region, where the hexagons forming the graphene honeycomb lattice are centered on the TOP sites of the Ir(111) surface.

However, by considering the height h with respect of the plane passing through the Ir(111) surface, some information is lost. For example, this approach does not consider the Ir surface buckling (~0.01 Å according to our calculations) and the different position of non-equivalent C atoms in the HCP and FCC regions with respect to the surface. As a matter of fact, in these regions one C atom is located ontop with respect to the surface Ir atom, while his C nearest neighbors are located above a threefold adsorption site and their distance from the closest Ir atom is different (3.30 Å vs 3.60 Å for C atoms in ontop and threefold sites in the HCP region). To include these aspect in our analysis, we considered the C-Ir distance between C atoms and the closest Ir atom from the Ir(111) surface. Fig. 2a shows the C atoms with different colors based on this distance. The C-Ir distance distribution is reported in Fig. 2b, which highlights the broadening around the average value of 3.56 Å, which is larger than the average height h due to simple geometric considerations.

We calculated the C 1s BE for each of the 200 C atoms in the moiré unit cell in the final-state approximation [35]. The results are shown in Fig. 3, highlighting the different BEs with a color scale: dark blue indicates higher BEs, while light blue indicates lower values, i.e., closer to the Fermi level. The color scale pattern recalls the one where the C atoms are colored based on the distance from the substrate (Fig. 2a). This
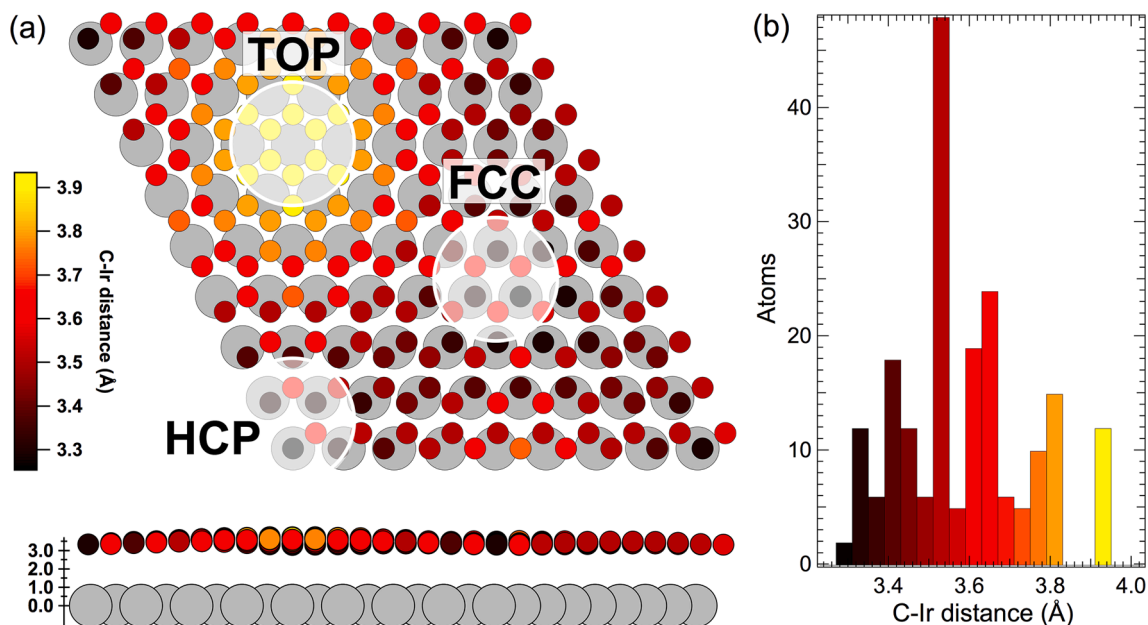
Fig. 2. (a) Top and side view of the simulated graphene/Ir(1 1 1) interface structure where the location of the TOP, FCC and HCP regions, described in the text, are indicated by circles. The color scale reflects the separation between the C atoms and the first-layer Ir atoms in the surface beneath. (b) Distribution of the C-Ir distance in the moiré cell.
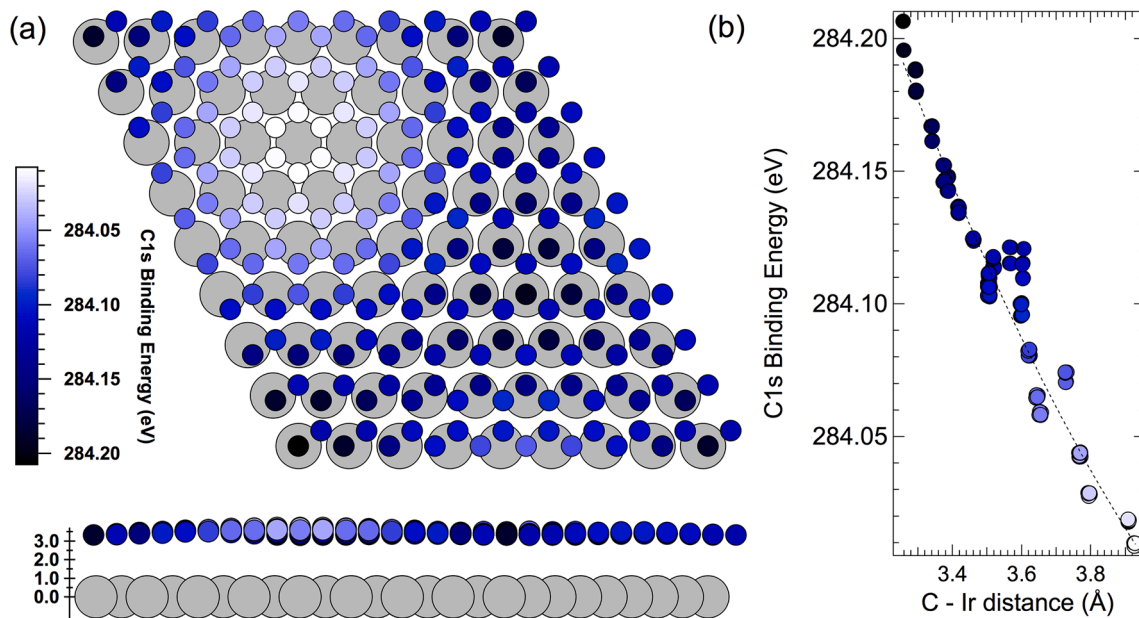

Fig. 3. (a) Top and side view of the DFT calculated C 1s binding energy of non-equivalent carbon atoms in the moiré graphene/Ir(1 1 1) unit cell. The color scale reflects the binding energy values. (b) C 1s binding energy dependence on the C-Ir distance.

suggests that, as happens in the case of graphene/Re(0001) and Ru (0001), also on graphene/Ir(1 1 1) the C 1s BEs depend on the distance from the substrate, in good agreement with previous calculations [21]. The energy dispersion of 200 meV among the different atoms in the unit cell is considerably smaller than in the case of graphene/Re(0001), where energy difference between atoms in the FCC and TOP regions is higher than 1.4 eV [19]. The narrow dispersion of the binding energies makes it impossible to experimentally distinguish spectral components due to different degree of interaction, in good agreement with the fact that usually the C 1s spectrum for this system can be fitted with a single DS component with a FWHM between 0.25 and 0.30 eV.

3.3. DFT-based data analysis of the C 1 s experimental spectrum.

The first attempt for the analysis of the C 1s graphene/Ir(1 1 1) spectrum consisted in a fit with 200 DS components, all having the same intensity and with BEs determined by the DFT calculations which included final-state effects. The G and L widths were fixed to be the same for all the components, and the same goes for the asymmetry parameter α. The fitting curve that minimizes the χ^2 has G and L values of 79 and 141 meV, respectively. The 41 % lower value of the G width compared to the fit with a single component arises from the fact that we are disentangling the contribution arising from the non-equivalent atoms in the unit cell from the overall fitting line. Nevertheless, the G value of 79

meV is still larger than the broadening due to the experimental resolution because of the contribution from the phonon broadening. The asymmetry parameter ($\alpha =0.074$) does not change appreciably for the fit with 200 components.

The result of this analysis, although it is in quite good agreement with the experimental results, shows a slightly higher reduced-χ^2 (12.02, i.e. $+18\%$ with respect to the value with a single DS) with respect to the one obtained using a single component (blue curve in Fig. 4). This indicates that the introduction of all the different 200 components arising from non-equivalent carbon atoms is not sufficient to improve the fit. To overcome this problem, we decided to analyze the C 1s spectrum allowing a dispersion of the Lorentzian widths of each atom in the cell. In particular, the L_j width of the j-th atom ($j = 1, \cdots, 200$) follows an exponential law $L_j = A\exp(-Bd_j)$, where d_j is its distance from the closest Ir atom, while A and B are constants that were used as fitting parameters. In this case The intensity of each Doniach-Šunjić convoluted with a Gaussian has been normalized using the term $L^{(1-\alpha)}$ to obtain a value proportional to the area under each peak.

This approach led to a considerable increase in the quality of the fit (red curve in Fig. 4), with the reduced-χ^2 (5.45) that is now 55 % smaller than in the case where 200 DS with equal Lorentzian are considered. The L widths range from 93 to 217 meV, i.e., with a difference included between -34% and $+53\%$ with respect to the value obtained using a single value of Lorentzian ($L = 141$ meV) [31]. The value of the asymmetry parameter of 0.052 is close the one found in the case of monolayer
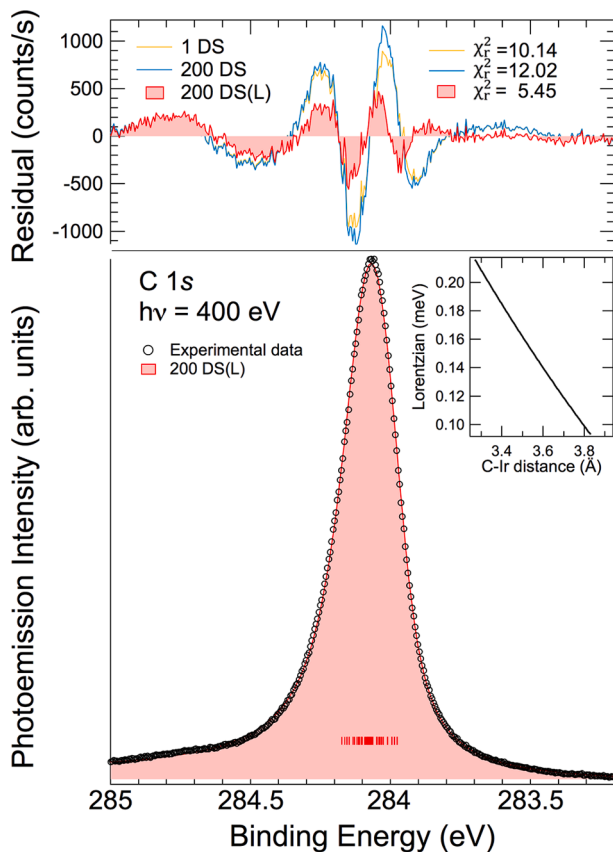

Fig. 4. Same C 1s spectrum reported in Fig. 1 together with the result of the fit performed using a 200 DS function with a functional dependence of the Lorentzian width on the C-Ir distance (red solid line). The values assumed by the Lorentzian width are reported in the panel. In the top panel the residual of the fit performed using a single DS (orange curve), 200 DS with same Lorentzian (blue curve) and 200 DS components with a functional dependence of L (red curve) are reported. The binding energy values of the 200 components are reported as bar codes in the bottom part. The values of the reduced-χ^2 are also reported.

suspended graphene, equal to 0.095 [36].

4. Discussion

The fact that the reduced-χ^2 improves when a functional dependency is added to the 200 DS(L) components on the C – Ir distance brings up the question on why the L width should have a similar behavior. In particular, it is crucial to understand why the L width increases when the C – Ir distance decreases. The L component in the DS lineshape is related through the uncertainty principle to the lifetime τ of the core–hole that is generated by the photoemission process ($L\tau > \hbar/2$). In particular, the core–hole lifetime decreases (and L increases) for an increasing probability of electron transitions to fill the hole from higher electronic levels. In the case of light elements such as C, these transitions are dominated by the non-radiative Auger process, where a valence electrons V_1 is de-excited to fill the K state and the transition energy is imparted to a second valence electron V_2 which is emitted from the sample [37]. For graphene, the lifetime τ of the excited state is proportional to the inverse of the sum of all partial transition rates to various final states. More specifically, the KVV transition depends on the occupancy of the σ e π states in the valence band in the vicinity of the core hole. Although this occupancy is the same for all the C atoms in a freestanding graphene layer, the interaction with the substrate is expected to induce some modifications on the electronic structure of the valence band. For instance, in the case of graphene/Ru(0001), a system where the graphene layer is highly corrugated, the density of state close to the Fermi level for 2 s and 2p electrons (σ e π bands) is affected based on the region of the moiré cell where the calculations are performed. Despite the lower corrugation of graphene/Ir(1 1 1), a similar effect could arise also for this system, with potential repercussions also on the core–hole lifetime of different C atoms which is linked to the density of those states that are energetically closer to the C 1s core.

In this regard, we calculated the density of p and s states for each C atom in the moiré cell of the graphene layer. To improve the quality of the results, the calculations were performed including 512 K points in the Brillouin zone. Fig. 4a shows the s (blue) and p (red) states distribution for the atoms with the lowest (dark colors) and highest (light colors) C – Ir distance in the unit cell. The two curves are clearly different in the lowest energy region, away from the Fermi level. Both the s and p density of state in this region is higher when C atoms are closer to the substrate. To prove that this result is not limited exclusively to the two atoms at the edges of the distribution, but it can be extended for all the C atoms in the graphene layer, in Fig. 4b we report the co-ordinate of the p and s band barycenter as a function of the C – Ir distance. The inverse relationship between the coordinate of the barycenter with respect to the C – Ir distance agrees with the trend observed for the L widths in the fitting analysis. The shorter the C – Ir distance, the closer (energetically speaking) the barycenter of the d and s bands are to the core–hole. This facilitates the de-excitation process and decreases the core–hole lifetime and, therefore, increases the L width. On the contrary, for the atoms further away from the substrate, the barycenter of the d and s bands shifts towards the Fermi level, resulting in a lower deexcitation probability, larger core–hole lifetime and smaller L width. A more rigorous analysis on the probability of the transition between different electron levels would be required to obtain a more quantitative analysis of the two trends, but such analysis falls outside the scope of this work, and it is greatly complicated by the size of the unit cell used for the calculations, which, considering both C and Ir, counts a total of 524 atoms.

It is interesting to compare the C 1s lifetime width we obtained in our experiment with the values measured for a variety of carbon-based molecules in gas-phase. The minimum value of 75 meV from our experiment is close to what has been found in the case of CF_4 (73 ± 5 meV), while larger values ranging from 96 to 107 meV have been reported for CO, C_2H_2 and C_2H_4 [38]. A larger number of accessible states for the de-excitation corresponds to a shorter lifetime of the core hole,
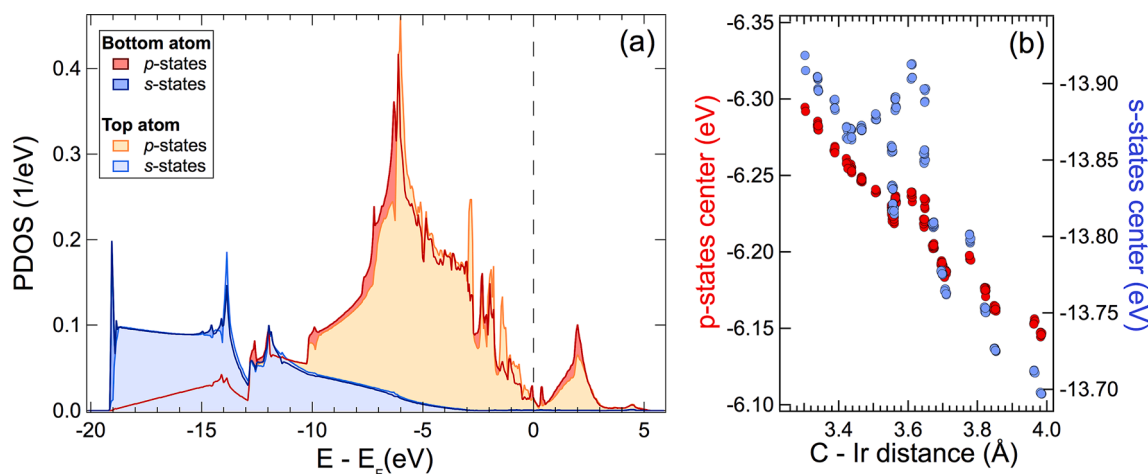
Fig. 4a. (a) Calculated projected density of s- (blue) and p-states (red) for the C atoms with the lowest (dark colors) and highest (light colors) C – Ir distance in the moiré unit cell. **(b)** Values of the s- and p-states center for all the C atoms in the moiré unit cell as a function of the C – Ir distance.

and this is the main reason why C atoms in a molucule show a decreased core hole lifetime with respect to the atoms of the same species in a graphene monolayer.

5. Conclusions

In the present work we have shown how, also in the case of a graphene-metal interface with a low interaction, the C 1s core levels can be influenced by the presence of the substrate. This is proven by the increased quality of the experimental analysis when it is performed introducing 200 spectral components, with DFT calculated C 1s binding energies, originating from the 200 non-equivalent C atoms composing the moiré unit of graphene on Ir(1 1 1). The best fit is obtained when a functional dependency of Lorentzian width on the C – Ir distance is introduced. Our theoretical calculations suggest that this result has to do with the different s and p density of states in the minimum of the valence band, away from the Fermi level and closer to the C 1s core level, which affects the probability of an Auger transition to fill the core–hole generated by the photoemission process. This result highlights how an apparently single-component and of simple-interpretation spectrum may involve several physical phenomena which, in first instance, could results hidden, but that, if adequately handled, allow to obtain new information from the system and a more accurate comparison with the experimental results.

CRediT authorship contribution statement

Cecilia Botta: Formal analysis, Data curation, Investigation, Writing – review & editing. **Federico Loi:** Formal analysis, Investigation, Writing – review & editing. **Dario Alfè:** Formal analysis, Investigation, Writing – review & editing. **Alessandro Baraldi:** Conceptualization, Investigation, Supervision, Writing – original draft.

Declaration of Competing Interest

The authors declare that they have no known competing financial interests or personal relationships that could have appeared to influence the work reported in this paper.

Data availability

Data will be made available on request.

References

[1] K. Siegbahn, Electron spectroscopy - an outlook, J. Electron Spectrosc. Relat. Phenom. 5 (1974) 3–97.

[2] A. Gupta, T. Sakthivel, S. Seal, Recent development in 2D materials beyond graphene, Prog. Mater Sci. 73 (2015) 44–126.

[3] K.S. Novoselov, A. Mishchenko, A. Carvalho, A.H. Castro Neto, 2D materials and van der Waals heterostructures, Science 353 (2016) aac9439.

[4] L. Bignardi, P. Lacovig, R. Larciprete, D. Alfè, S. Lizzit, A. Baraldi, Exploring 2D materials at surfaces through synchrotron-based core-level photoelectron spectroscopy, Surf. Sci. Rep. 78 (2023), 100586.

[5] Citation database Scopus Elsevier: TITLE (graphene) AND ALL ("x-ray photoelectron spectroscopy"), in: 17 August 2023.

[6] D. Geng, S. Yang, Y. Zhang, J. Yang, J. Liu, R. Li, T.-K. Sham, X. Sun, S. Ye, S. Knights, Nitrogen doping effects on the structure of graphene, Appl. Surf. Sci. 257 (2011) 9193–9198.

[7] D. Yang, A. Velamakanni, G. Bozoklu, S. Park, M. Stoller, R.D. Piner, S. Stankovich, I. Jung, D.A. Field, C.A. Ventrice, R.S. Ruoff, Chemical analysis of graphene oxide films after heat and chemical treatments by X-ray photoelectron and Micro-Raman spectroscopy, Carbon 47 (2009) 145–152.

[8] R. Larciprete, S. Fabris, T. Sun, P. Lacovig, A. Baraldi, S. Lizzit, Dual Path Mechanism in the Thermal Reduction of Graphene Oxide, J. Am. Chem. Soc. 133 (2011) 17315–17321.

[9] U.A. Schröder, E. Grånäs, T. Gerber, M.A. Arman, A.J. Martínez-Galera, K. Schulte, J.N. Andersen, J. Knudsen, T. Michely, Etching of graphene on Ir(111) with molecular oxygen, Carbon 96 (2016) 320–331.

[10] A.T. N'Diaye, S. Bleikamp, P.J. Feibelman, T. Michely, Two-Dimensional Ir Cluster Lattice on a Graphene Moiré on Ir(111), Phys. Rev. Lett. 97 (2006).

[11] C. Busse, P. Lazić, R. Djemour, J. Coraux, T. Gerber, N. Atodiresei, V. Caciuc, R. Brako, A.T. N'Diaye, S. Blügel, J. Zegenhagen, T. Michely, Graphene on Ir(111): Physisorption with Chemical Modulation, Phys. Rev. Lett. 107 (2011).

[12] F. Presel, N. Jabeen, M. Pozzo, D. Curcio, L. Omiciuolo, P. Lacovig, S. Lizzit, D. Alfè, A. Baraldi, Unravelling the roles of surface chemical composition and geometry for the graphene–metal interaction through C1s core-level spectroscopy, Carbon 93 (2015) 187–198.

[13] R. Balog, B. Jørgensen, L. Nilsson, M. Andersen, E. Rienks, M. Bianchi, M. Fanetti, E. Lægsgaard, A. Baraldi, S. Lizzit, Z. Sljivancanin, F. Besenbacher, B. Hammer, T. G. Pedersen, P. Hofmann, L. Hornekær, Bandgap opening in graphene induced by patterned hydrogen adsorption, Nat. Mater. 9 (2010) 315–319.

[14] S. Lizzit, G. Zampieri, L. Petaccia, R. Larciprete, P. Lacovig, G. Emile, A. Bihlmayer, P.H. Baraldi, Band dispersion in the deep 1s core level of graphene, Nat. Phys. 6 (2010) 345–349.

[15] A.B. Preobrajenski, M.L. Ng, A.S. Vinogradov, N. Mårtensson, Controlling graphene corrugation on lattice-mismatched substrates, Phys. Rev. B 78 (2008), 073401.

[16] D. Pacilé, S. Lisi, I. Di Bernardo, M. Papagno, L. Ferrari, M. Pisarra, M. Caputo, S. K. Mahatha, P.M. Sheverdyaeva, P. Moras, P. Lacovig, S. Lizzit, A. Baraldi, M. G. Betti, C. Carbone, Electronic structure of graphene/Co interfaces, Phys. Rev. B 90 (2014), 195446.

[17] C.C. Silva, M. Iannuzzi, D.A. Duncan, P.T.P. Ryan, K.T. Clarke, J.T. Küchle, J. Cai, W. Jolie, C. Schlueter, T.-L. Lee, C. Busse, Valleys and Hills of Graphene on Ru (0001), J. Phys. Chem. C 122 (2018) 18554–18561.

[18] H. Vita, S. Böttcher, P. Leicht, K. Horn, A.B. Shick, F. Máca, Electronic structure and magnetic properties of cobalt intercalated in graphene on Ir(111), Phys. Rev. B 90 (2014), 165432.

[19] E. Miniussi, M. Pozzo, A. Baraldi, E. Vesselli, R.R. Zhan, G. Comelli, T.O. Menteş, M.A. Niño, A. Locatelli, S. Lizzit, D. Alfè, Thermal Stability of Corrugated Epitaxial Graphene Grown on Re(0001), Phys. Rev. Lett. 106 (2011).

[20] D. Alfè, M. Pozzo, E. Miniussi, S. Günther, P. Lacovig, S. Lizzit, R. Larciprete, B. S. Burgos, T.O. Menteş, A. Locatelli, A. Baraldi, Fine tuning of graphene-metal adhesion by surface alloying, Sci. Rep. 3 (2013).

[21] J. Knudsen, P.J. Feibelman, T. Gerber, E. Grånäs, K. Schulte, P. Stratmann, J. N. Andersen, T. Michely, Clusters binding to the graphene moiré on Ir(111): X-ray photoemission compared to density functional calculations, Phys. Rev. B 85 (2012).

[22] S. Doniach, M. Sunjic, Many-electron singularity in X-ray photoemission and X-ray line spectra from metals, J. Phys. C Solid State Phys. 3 (1970) 285.

[23] M. Bianchi, D. Cassese, A. Cavallin, R. Comin, F. Orlando, L. Postregna, E. Golfetto, S. Lizzit, A. Baraldi, Surface core level shifts of clean and oxygen covered Ir(111), New J. Phys. 11 (2009), 063002.

[24] S. Lizzit, A. Baraldi, High-resolution fast X-ray photoelectron spectroscopy study of ethylene interaction with Ir(111): From chemisorption to dissociation and graphene formation, Catal. Today 154 (2010) 68–74.

[25] V. Despoja, M. Šunjić, Theory of core-level spectra in x-ray photoemission of pristine and doped graphene, Phys. Rev. B 88 (2013).

[26] G. Kresse, J. Furthmüller, Efficient iterative schemes for ab initio total-energy calculations using a plane-wave basis set, Phys. Rev. B 54 (1996) 11169–11186.

[27] I. Hamada, van der Waals density functional made accurate, Phys. Rev. B 89 (2014), 121103.

[28] P.E. Blöchl, Projector augmented-wave method, Phys. Rev. B 50 (1994) 17953–17979.

[29] G. Kresse, D. Joubert, From ultrasoft pseudopotentials to the projector augmented-wave method, Phys. Rev. B 59 (1999) 1758–1775.

[30] J.P. Perdew, K. Burke, M. Ernzerhof, Generalized Gradient Approximation Made Simple, Phys. Rev. Lett. 77 (1996) 3865–3868.

[31] M. Pozzo, D. Alfè, P. Lacovig, P. Hofmann, S. Lizzit, A. Baraldi, Thermal Expansion of Supported and Freestanding Graphene: Lattice Constant versus Interatomic Distance, Phys. Rev. Lett. 106 (2011).

[32] I. Wendt, C. Carl, The statistical distribution of the mean squared weighted deviation, Chemical Geology: Isotope Geoscience Section 86 (1991) 275–285.

[33] S. Runte, P. Lazić, C. Vo-Van, J. Coraux, J. Zegenhagen, C. Busse, Graphene buckles under stress: An x-ray standing wave and scanning tunneling microscopy study, Phys. Rev. B 89 (2014), 155427.

[34] J. Coraux, A. T N'Diaye, M. Engler, C. Busse, D. Wall, N. Buckanie, F.-J. Meyer zu Heringdorf, R. van Gastel, B. Poelsema, T. Michely, Growth of graphene on Ir(111), New J. Phys., 11 (2009) 023006.

[35] S. Lizzit, A. Baraldi, A. Groso, K. Reuter, M.V. Ganduglia-Pirovano, C. Stampfl, M. Scheffler, M. Stichler, C. Keller, W. Wurth, D. Menzel, Surface core-level shifts of clean and oxygen-covered Ru(0001), Phys. Rev. B 63 (2001).

[36] T. Susi, M. Scardamaglia, K. Mustonen, M. Tripathi, A. Mittelberger, M. Al-Hada, M. Amati, H. Sezen, P. Zeller, A.H. Larsen, C. Mangler, J.C. Meyer, L. Gregoratti, C. Bittencourt, J. Kotakoski, Intrinsic core level photoemission of suspended monolayer graphene, Physical Review Materials 2 (2018).

[37] A.A. Galuska, H.H. Madden, R.E. Allred, Electron spectroscopy of graphite, graphite oxide and amorphous carbon, Appl. Surf. Sci. 32 (1988) 253–272.

[38] C. Nicolas, C. Miron, Lifetime broadening of core-excited and -ionized states, J. Electron Spectrosc. Related Phenom. 185 (2012) 267–272.